Biosensors and Bioelectronics 132 (2019) 136–142

Contents lists available at ScienceDirect

Biosensors and Bioelectronics

journal homepage: www.elsevier.com/locate/bios

Lab-on-a-screen-printed electrochemical cell for drop-volume voltammetric screening of flunitrazepam in untreated, undiluted alcoholic and soft drinks

Fotini Tseliou[a], Periklis Pappas[b], Konstantinos Spyrou[c], Jan Hrbac[d], Mamas I. Prodromidis[a,*]

[a] Department of Chemistry, University of Ioannina (UOI), Ioannina 45110, Greece
[b] Department of Pharmacology, Faculty of Medicine, UOI, Ioannina, Greece
[c] Department of Materials Science and Engineering, UOI, Ioannina 45110, Greece
[d] Department of Chemistry, Masaryk University, 62500 Brno, Czech Republic

ARTICLE INFO

Keywords:
Flunitrazepam
Rohypnol®
Drug-facilitated sexual assault
Date-rape drugs
Screen-printed sparked electrodes
Point-of-need voltammetric sensors

ABSTRACT

Flunitrazepam, also known as “Rohypnol” or “Rophy” among other trade and street names, is an extremely potent benzodiazepine that is prescribed to treat severe insomnia. Due to these attributes, flunitrazepam, when is surreptitiously administered to an alcoholic or soft drink, is associated with “drug-facilitated sexual assault”. We report here for the first time, a low cost lab-on-a-screen-printed electrochemical cell (SPC) based on iron-sparked graphite working electrode modified with glucose oxidase (GOx) and glucose hydrogel droplets (GluHD) for the detection of flunitrazepam. Iron-spark modification increases the response of the sensor by ca. 3-fold compared with that of the plain electrode, while an in situ deoxygenation process, based on GOx-glucose enzyme reaction, depletes dissolved oxygen. As a result, the method enables interference free voltammetric measurements of the electro reduction of the nitro group of flunitrazepam at ca. −0.71 to −0.78 V vs. Ag printed pseudo reference electrode depending on the sample's matrix, and the detection of the drug at the sub-millimolar level. GOx/GluHD-FeSPC was directly applied to the drop-volume (~60 μL) detection of flunitrazepam to a wide range of untreated and undiluted spiked samples (Pepsi cola®, Vodka, Whisky, Tequila, Gin, and Rum) of different acidity (pH 2.3–8.4), and alcohol content up to 40% v/v. Data demonstrate the excellent performance of the sensor for point-of-need screening of flunitrazepam and suggest that GOx/GluHD-FeSPC holds promise as an effective analytical tool to prevent phenomena of covert drug administration.

1. Introduction

Rohypnol® is a trade name for flunitrazepam, a Schedule IV central nervous system depressant that belongs to benzodiazepines (U.S. Department of justice, 2017). Flunitrazepam is also marketed with other trade name products (Roipnol®, Fluninoc®, Silece®, Hipnosedon®, Nervocuril® etc.) and it is legally prescribed in more than 60 countries in Europe, Africa, Latin America, Middle East, Asia, and Australia to treat severe insomnia (Mattila and Larni, 1980). Flunitrazepam, however, is also illegally found in countries in which its medical use is not approved. In the United States and elsewhere, flunitrazepam is smuggled as illegally produced tablets or legally manufactured preparations and it is used as a recreational drug (Wu et al., 2006). Flunitrazepam is also misused to “drug-facilitated sexual assaults” (DFSA), i.e. to physically and psychologically incapacitate a person, usually women, targeted for sexual assault. In these instances, flunitrazepam is surreptitiously administered to an alcoholic or non-alcoholic drink of an unsuspecting victim to prevent resistance to sexual assault (Dinis-Oliveira and Magalhães, 2013; Mullins, 1999; Schwartz, 1998; U.S. Department of justice, 2017; Weir, 2001). Flunitrazepam intake, especially when it is combined with alcohol, results in the victim being unable to recall the episode, thus making difficult to report it or to ask timely sexual assault forensic examination (Beynon et al., 2008; Dinis-Oliveira and Magalhães, 2013; LeBeau and Mozayani, 2001). Due to this fact, along with rape taboo, even in developed countries (McNeill, 2018), and rape victims reluctance to report the event in the aftermath of past stories where rape victims were charged with lying and prosecuted (Miller and Armstrong, 2018), DFSA is an unreported crime. According to the British Crime Survey in only 12% of sexual assault incidents, victims asked the police to become involved (Beynon et al., 2008; Walby and Allen, 2004).

Covert drug administration however, is not only associated with DFSA and flunitrazepam; robberies, homicides, fatal street accidents (LeBeau and Mozayani, 2001), as well as other substances, less

* Corresponding author.
E-mail address: mprodrom@uoi.gr (M.I. Prodromidis).

https://doi.org/10.1016/j.bios.2019.03.001
Received 9 February 2019; Received in revised form 3 March 2019; Accepted 5 March 2019
Available online 05 March 2019
0956-5663/

"popular" than flunitrazepam regarding its use as "date-rape drug", such as gamma hydroxybutyric acid and ketamine have also been reported (Amir and Waisman, 2006; Dasgupta, 2017; Dinis-Oliveira and Magalhães, 2013).

World Health Organization identifies the increasing implicative role of "date-rape drugs" in incidents of sexual violence (WHO, 2003), while in the light of concern for the increasing number of DFSAs, the U.S. Congress passed the Drug-Induced Rape Prevention and Punishment Act (Drug-Induced Rape Prevention and Punishment Act, 1996; Executive Office of the President, 2003), which imposes stiff sentences for DFSAs and for the importation and distribution of flunitrazepam. In 2006, the Parliamentary Assembly of the Council of Europe took also steps in order to raise the public's awareness to sexual assaults linked to "date-rape drugs" (Council of Europe, 2006).

When is dissolved in drinks, flunitrazepam is odorless and tasteless, while legally manufactured tablets when mixed in drinks dye the liquid blue (generic versions of the drug may not contain the blue dye). Once it ingested, its action begins after 20–30 min, peaked at 2 h and lasts up to 8 h (Mattila and Larni, 1980).

For the determination of flunitrazepam and its metabolites (mainly 7-aminoflunitrazepam) in various biological samples a number of analytical techniques such as, liquid chromatography coupled with different detectors [optical (Wilhelm et al., 2000), electrochemical (Wilhelm et al., 2000), or mass spectrometric (D'Aloise and Chen, 2012)], gas chromatography-mass spectroscopy (Samyn et al., 2002), sweeping micellar electrokinetic chromatography (Huang et al., 2006), capillary electrophoresis (Baciu et al., 2015), as well as various commercially available immunoassay test kits (Barrett et al., 1999) have been developed. For the determination of flunitrazepam in beverages, Leesakul et al. (Leesakul et al., 2012) proposed a fluorescence spectroscopy method which, however, is applicable only in colorless spirits. Another approach based on high-performance liquid chromatography coupled with a dual electrode detector enables the determination of flunitrazepam in sample's extracts (Honeychurch and Hart, 2008), while a bench-top method for the direct determination of flunitrazepam in spiked beverages was demonstrated by Webb et al. (Webb et al., 2007) by using capillary zone electrophoresis.

Despite the fact that the most effective way to prevent DFSAs is associated with simple rules that have to be applied by consumers themselves, such as ordering sealed drinks, or obtaining a fresh one after leaving the drink unattended (Weir, 2001), consumers ask for a practical way to check the safety of their drinks. In this regard, easy-to-perform screening kits or sensors that would enable the point-of-need detection of flunitrazepam by non-trained individuals are highly desired.

To best of our knowledge, no commercial kit has been approved yet (Beynon et al., 2006, 2008), while the literature on the development of electrochemical sensors, which exhibit inherent advantage over optical methods (Leesakul et al., 2012), or color changing drug warning drinkwares (DrinkSavvy®, 2018) for the determination of flunitrazepam is extremely little (Garcia-Gutierrez et al., 2013; Garcia-Gutierrez and Lledo-Fernandez, 2013; Smith et al., 2013). Garcia-Gutierrez and Lledo-Fernandez have reported the electrochemical determination of flunitrazepam in degassed solutions by using plain (Garcia-Gutierrez et al., 2013) or graphene-modified (Garcia-Gutierrez and Lledo-Fernandez, 2013) graphite screen-printed electrodes, while the method developed by Smith et al. (2013) demonstrates the electrochemical sensing of flunitrazepam only to acidic (pH 2), low content alcohol (< 5% v/v) samples by using graphite screen-printed electrodes. Aforementioned electrochemical methods (Garcia-Gutierrez et al., 2013; Garcia-Gutierrez and Lledo-Fernandez, 2013; Smith et al., 2013) employ voltammetric measurements of an electrochemically generated –NO/NH-OH redox couple, which as it is not originally present in flunitrazepam, the assay protocol requires a cathodic polarization step, aiming at electro reduction of the $–NO_2$ group of flunitrazepam to NH-OH, to be preceded. Crucially however, with increasing pH values the formal potential of the –NO/NH-OH redox couple shifts to cathodic potential values (Smith et al., 2013) where oxygen interference might not to be negligible. In addition, the cathodic treatment itself results in the formation of oxygen bubbles. Especially under quiescent conditions intended for point-of-care applications, it is expected that oxygen evolution partially blocks the electrode surface, thus impairing the response of the sensor.

Herein, we report a straightforward method for the electro reduction of the $–NO_2$ group of flunitrazepam and propose a simple yet effective approach to eliminate oxygen interference. The method is based on a disposable lab-on-a-screen-printed electrochemical cell that enables the drop-volume detection of flunitrazepam to undiluted, untreated and non-deoxygenated real-world samples. Three simple modification steps, that is, iron-sparking of the working electrode, immobilization of glucose oxidase (GOx) and application of glucose hydrogel droplets (GluHD) onto the screen-printed electrochemical cell, endow the desired properties for point-of-need applications. Sparked generated Fe_xO_y nanoparticles increase the sensitivity by ca. 3-fold, while an in situ deoxygenation process based on GOx-glucose enzyme reaction depletes dissolved oxygen and enables the application of the sensor to non-deoxygenated samples. To the best of our knowledge, this work demonstrates for the first time, the direct, drop-volume detection of flunitrazepam to a wide range of untreated, undiluted alcoholic and soft drinks of different acidity (pH 2.3–8.4) and alcohol content up to 40% v/v.

2. Material and methods

2.1. Materials

Flunitrazepam was purchased by LGC Standards Ltd under the license of the UK controlled drug export office. Rohypnol® 1 mg flunitrazepam tabs (Hoffman-La Roche) were supplied by the Department of Pharmacology of UOI. Glucose oxidase from *Aspergillus niger* (Type VII, ≥100 kU/g solid), sodium carboxymethyl cellulose (CMC) (M_w ~250 kDa) and D-(+)-glucose were Sigma-Aldrich products. The stock solution of glucose in water was used 24 h after its preparation and then stored at 4 °C. 0.1 M phosphate-buffered saline (PBS) pH 7 was used as electrolyte and for the preparation of enzyme solutions. Double-distilled water (DDW) was used throughout. Alcoholic and soft drinks were obtained by the local market.

2.2. Apparatus

Cyclic voltammetry (CV), differential pulse voltammetry (DPV) and electrochemical impedance spectrometry (EIS) measurements were conducted with the PGSTAT12/FRAII electrochemical analyzer (Metrohm Autolab). Batch experiments were performed in a single compartment three-electrode cell. Plain or iron-sparked single graphite screen-printed electrodes (denoted as SPE and FeSPE, respectively) were used as working electrode, and a Pt wire as auxiliary electrode. The reference electrode was a Ag/AgCl/3 M KCl (IJ Cambria) electrode. Electrochemical measurements for the detection of flunitrazepam in alcoholic and soft drinks were performed with an iron-sparked screen-printed 3-electrode electrochemical cell (FeSPC) consisting of graphite working and auxiliary electrodes, and a pseudo reference silver electrode. All potentials reported hereafter are quoted to the potential of these reference electrodes in each case.

Scanning electron microscopy (SEM) images and energy dispersive X-ray spectroscopy (EDX) analysis were performed on a JEOL JSM-6510LV microscope equipped with an INCA PentaFETx3 × -ray detector (Oxford Instruments) on Au-sputtered (Polaron SC7620 sputter coater) samples. X-ray photoelectron spectroscopy (XPS) measurements were applied under ultrahigh vacuum with a SPECS GmbH instrument equipped with a monochromatic MgKa source (hv = 1253.6 eV) and a Phoibos-100 hemispherical analyzer (Riman et al., 2017).

2.3. Electrochemical measurements

EIS spectra were recorded in 5 + 5 mM hexacyanoferrate(II)/(III) in 0.1 M PBS, pH 7 over the frequency range 0.1–10^5 Hz using an excitation amplitude of 10 mV (rms), superimposed on a DC potential of − 0.200 V. CVs were recorded at a scan rate of 0.1 V s^{-1}. DP voltammograms were recorded over the potential range from − 0.2 to − 1.1 V using the following waveform parameters: pulse amplitude, 0.05 V; step potential, 0.009 V; voltage step time, 0.05 s. Under these conditions the effective scan rate was 0.03 V s^{-1}.

2.4. Modification of graphite electrodes by sparking process

The sparking process was conducted at ambient conditions at 1.2 kV by using an in-house power supply (200–2000 V) consisting of a 10 kHz oscillator, transformer and 5-stage Cockroft–Walton multiplier. Power supply terminals were connected in parallel with a 2.2 nF capacitor and modification of the SPE was conducted by bringing into close proximity (< 1 mm) the two conductors, until the spark discharge occurred. By connecting the Fe wire (> 99.9%, Goodfellow) as cathode (−) and the graphite SPE (or the graphite working electrode of the 3-electrode electrochemical cell) as anode (+), a number of 30 sparking cycles were uniformly spaced across the carbon surface. A detailed description of the spark discharge process, which enables the generation of nanoparticles on the basis of an evaporation-condensation mechanism, is given in previous works (Riman et al., 2015). Details on the fabrication of graphite SPE and 3-electrode electrochemical cells are given in Kokkinos et al., 2015a and Kokkinos et al., 2015b, respectively.

2.5. Preparation of GOx/GluHD-modified FeSPC

GOx was physically absorbed onto FeSPC by applied 2 µL of 2 mg L^{-1} GOx in 0.1 M PBS pH 7. For the modification of the screen-printed electrochemical cell with GluHD, a 10.00 mL viscous solution 0.05% w/v CMC in DDW containing 0.1080 g glucose was prepared. The solution was stirred overnight and then a 10 µL aliquot was applied in portions in the space between the working and the auxiliary electrodes in order to avoid contact of polymer drops containing glucose with GOx-modified surface of the working electrode. GOx/GluHD-FeSPC were left to dry in air for at least 3 h at ambient conditions and then stored at 4 °C (Fig. 1).

2.6. Procedures

Measurements with aforementioned electrodes were conducted under the following conditions: i) SPEs or FeSPEs were examined in 30 mL deoxygenated standard solutions of flunitrazepam in 0.1 M PBS pH 7, ii) GOx-FeSPCs were examined in drop-volume (60 µL) standard solutions or samples spiked with known concentrations of flunitrazepam containing 10 mM glucose, and iii) GOx/GluHD-FeSPCs were examined as in (ii) in a totally reagentless mode, that is, without the addition of glucose. In detail, 60 µL of each real sample (plain or fortified with 10 µM flunitrazepam) were applied to the surface of GOx/GluHD-FeSPC, and after a waiting time 4–6 min (see Table S1), DP voltammograms over the potential range from − 0.2 to − 1.1 V is recorded. The first scan is not considered for analytical purposes (conditioning of the electrode). The reduction peak at ca. − 0.81 ± 0.02 V, depending on the matrix of the real sample, verifies the presence of flunitrazepam.

3. Results and discussion

3.1. Characterization of iron-sparked graphite screen-printed electrodes

CVs in Fig. 2A show that with respect to the plain graphite electrode, FeSPE exhibits increased hydrogen and oxygen evolution reactions during the cathodic and anodic voltage sweeps, respectively. The electrochemical properties between SPE and FeSPE are also significantly different with respect to their surface/electrolyte faradic impedimetric profile (Fig. 2A, inset graph) in 0.1 M PBS pH 7 containing 5 + 5 mM hexacyanoferrate(II)/(III). FeSPE exhibits a charge-transfer resistance (R_{ct}) of 2.4 kOhm, which is significantly lower compared with that at SPE (R_{ct} = 4.2 kOhm). The decrease of R_{ct} at FeSPC is attributed to the modification of graphite surface with highly conductive spark generated Fe_xO_y nanoparticles. Importantly, EIS data also demonstrate that the sparking process results in quite reproducible surfaces.

From the high resolution XPS spectrum of iron $2p_{3/2}$ (Fig. 2B) at FeSPE, three different chemical states of iron were identified. For comparison, the XPS spectrum of iron $2p_{3/2}$ at plain SPE is given in Fig. S1. The intriguing part is that no peaks corresponding to metallic iron (Fe°) are observed indicating the spontaneous oxidation of vaporized iron to various oxides (Fe_xO_y) due to the high plasma temperature during the sparking process and the oxidation of the so-formed iron nanodroplets by air (Riman et al., 2015, 2017; Tabrizi et al., 2009). The atomic percentage of iron in the sample was found to be as low as 0.3%, leading thus to a relatively noisy signal. The XPS peak acquired from the Fe material is deconvoluted to three peaks: the first peak centered at 709.2 eV is due to FeO compounds and corresponds to the 35% of the total amount of iron. The second peak (710.5 eV, 54%) is attributed to Fe_3O_4 (Graat and Somers, 1996), while the third peak (712.1 eV, 11%) is assigned to FeO_2 compounds (Bu et al., 2013). The ratios of Fe(II)/Fe (III) and Fe(II)/Fe(IV) redox states in the solid sparked nanodeposits were calculated 0.4 and 0.9, respectively.

SEM image illustrated in Fig. 2C shows the sparking prints as craters, sized ca. 200 µm in diameter, that essentially represent the Fe_xO_y rich areas on the electrode surface. The higher magnification SEM image in Fig. 2D displays the formation of sponge-like deposits consisted of Fe_xO_y sparked nanoparticles, sized ca. < 100 nm along with the rare presence of larger agglomerates, that have been uniformly distributed over the sparked surface as evidenced by elemental EDX mapping acquired across the examined area (Fig. S2). For comparison purposes, a SEM image of plain SPE at x5000 magnification is shown in the inset of Fig. 2C.

3.2. Electrocatalytic performance

In accordance with the CVs illustrated in Fig. 3A, during the first cathodic sweep of the voltage, SPE shows two reduction peaks centered at − 0.733 V (R1) and − 1.139 V (R2) V, while the following anodic sweep up to 0.750 V reveals an anodic peak at 0.405 V (O1), which triggers the appearance of a third reduction peak at − 0.281 V (R3)

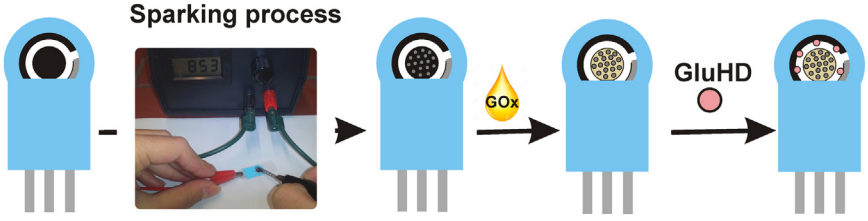

Fig. 1. Schematic representation of the preparation of GOx/GluHD-FeSPC. Gray dots represent the iron-sparked surface of the working electrode. GOx, glucose oxidase; GluHD, glucose hydrogel droplets.

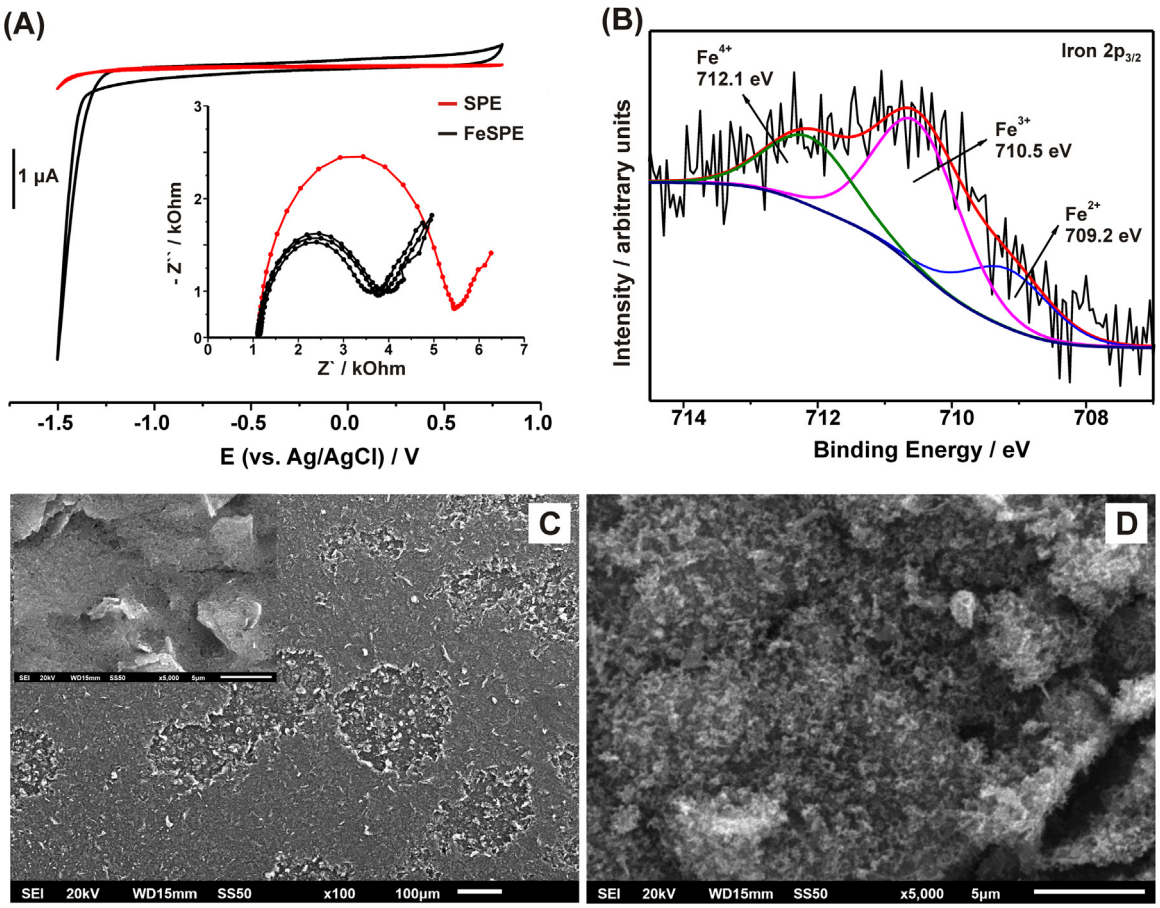

Fig. 2. (A) CVs of (red line) SPE and (black line) FeSPE at 0.1 M PBS, pH 7 at a scan rate 100 mVs^{-1}; Inset graph (2 A) shows the Nyquist plots of (red line) SPE and (black line) FeSPE in 5 + 5 mM hexacyanoferrate(II)/(III) in 0.1 M PBS, pH 7, and (B) XPS spectrum of iron $2p_{3/2}$ on FeSPE surface. SEM images of FeSPE showing (C) spark prints and (D) sponge-like spark generated Fe_xO_y deposits. Inset graph (2 C): SEM image of plain SPE at x5000 magnification (For interpretation of the references to color in this figure legend, the reader is referred to the web version of this article).

during the second cathodic scan. Considering the magnitude of R1, R2 peaks and previous literature (Bermejo et al., 1993; Núñez-Vergara et al., 1997; Oelshlager, 1983), the peak R1 corresponds to the reduction of the nitro group ($–NO_2$) of flunitrazepam to hydroxylamine (–NH-OH), according to a $4\,H^+/4e^-$ mechanism, and peak R2 to the $2\,H^+/2e^-$ reduction of the 4,5-azomethine (–N = C <) double bond

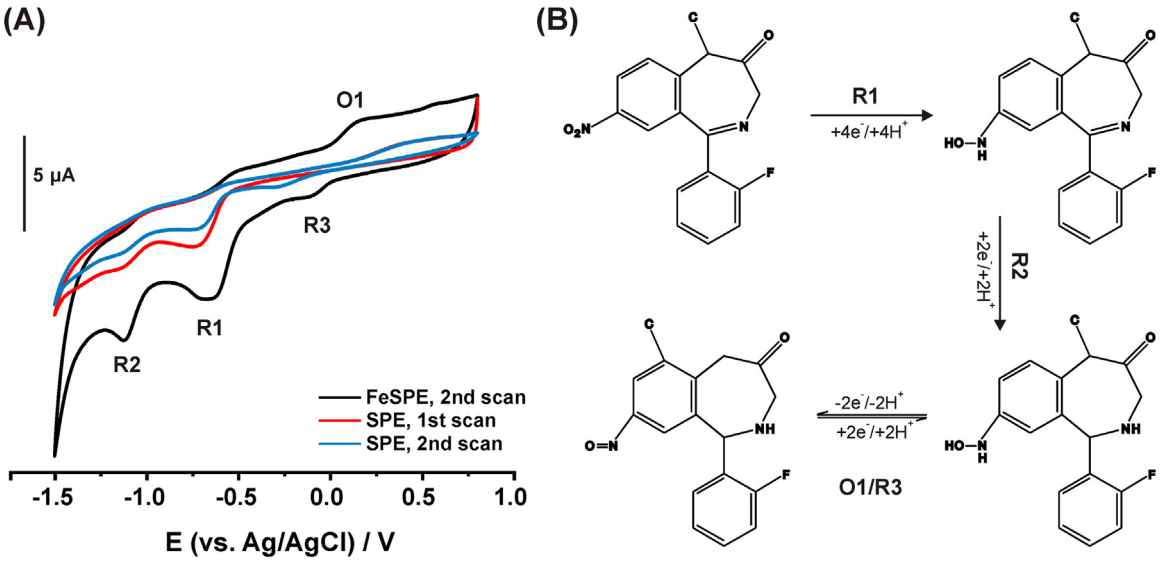

Fig. 3. (A) CVs of (red line: 1st scan; blue line, 2nd scan) SPE and (black line, 2nd scan) FeSPE in 5 μM flunitrazepam in 0.1 M PBS pH 7. Scan rate, 0.1 $V\,s^{-1}$. (B) Tentative mechanism for the electrochemical behavior of flunitrazepam (For interpretation of the references to color in this figure legend, the reader is referred to the web version of this article).

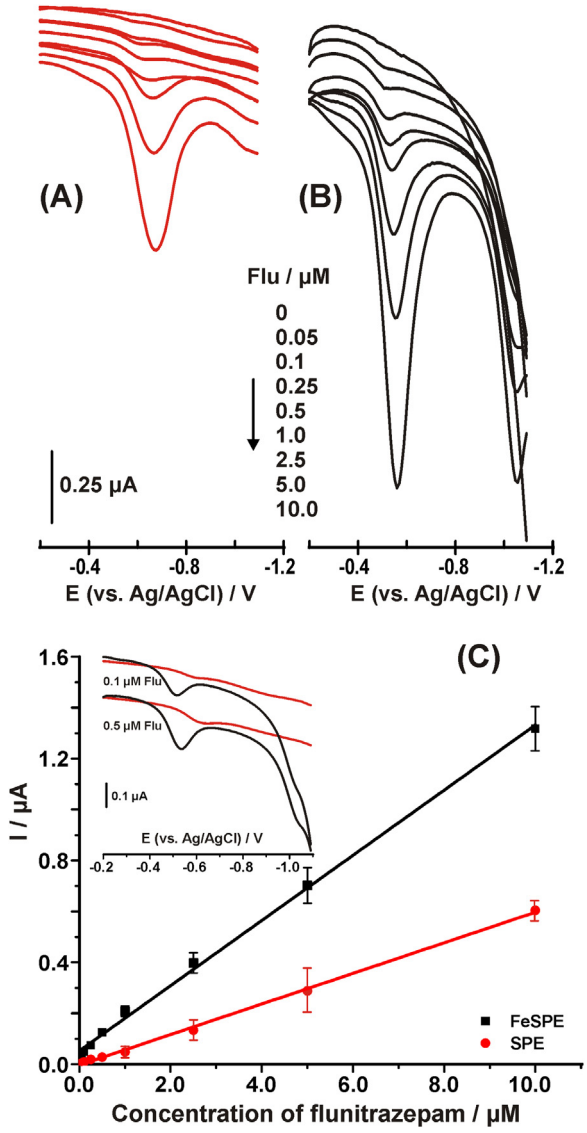

Fig. 4. DP voltammograms at (A) plain SPE, (B) sparked FeSPE over the concentration range from 0.05 to 10 μM flunitrazepam and (C) the respective calibration plots. Inset graph shows the comparative voltammetric responses of (red line) plain and (black line) sparked FeSPE in the presence of 0.1 and 0.5 μM flunitrazepam in deoxygenated 0.1 M PBS pH 7; Flu, flunitrazepam (For interpretation of the references to color in this figure legend, the reader is referred to the web version of this article).

(Fig. 3B).

The semi reversible pair of peaks O1/R3 is attributed to the redox transition of the hydroxylamine produced at R1 to a nitroso species and the reduction of it back to hydroxylamine (–NH-OH ↔ –NO) (Fig. 3B). Comparing the CV scans at SPE and FeSPE, it can be inferred that sparked generated Fe_xO_y nanoparticles endow FeSPE with enhanced electrocatalytic properties leading to redox transitions of higher peak magnitude and improved reversibility of O1/R3 redox couple. Potential peak separation, $\Delta E_p = |E_{p(O1)} - E_{p(R3)}|$, drops from 0.686 V at SPE to 0.258 V at FeSPE.

Enhanced electrocatalytic properties of FeSPE are also reflected to their detection capabilities to flunitrazepam. DP voltammograms at SPE (Fig. 4A) and sparked FeSPE (Fig. 4B) over the concentration range from 0.05 to 10 μM flunitrazepam along with the respective calibration plots (Fig. 4C) demonstrate that spark generated Fe_xO_y nanoparticles promote the electro reduction of the $–NO_2$ group of flunitrazepam leading to ca. 3-fold increase of the voltammetric response. Facile

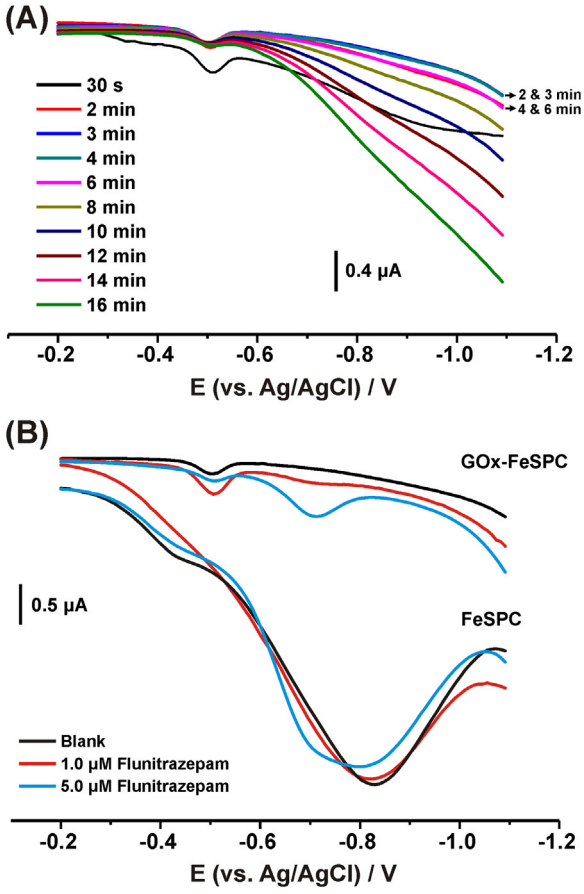

Fig. 5. (A) DP voltammograms of GOx-FeSPC at various time intervals after the application of 60 μL non-deoxygenated 0.1 M PBS pH 7 containing 10 mM glucose. (B) DP voltammograms of FeSPC and GOx-FeSPC in non-deoxygenated 0.1 M PBS pH 7 containing 10 mM glucose and 1 and 5 μM flunitrazepam.

electro catalytic reduction of flunitrazepam at FeSPE is also evident by the cathodic shift of the potential peak as depicted at Fig. 4C, inset graph showing the comparative response of SPE and FeSPE at two selected concentrations of flunitrazepam. For a signal-to-noise ratio of 3 (S/N 3), the limits of detection (LOD) were found to be 0.03 and 0.015 μM flunitrazepam, respectively, which compare favorably to previous works based on screen-printed electrodes (Table S2).

3.3. In-situ enzymatic depletion of dissolved oxygen

FeSPC were further modified with physically absorbed GOx, and, in the presence of added glucose, the kinetics of oxygen depletion at drop-volume standards and real-world samples was investigated. For the purposes of this study, various experimental parameters such as the concentration of the added glucose (Fig. S3) and the concentration of the 2 μL GOx solution applied on FeSPC (Fig. S4) were optimized. Optimal values were 10 mM and 2 mg mL^{-1}, respectively. The extra reduction peak at −0.5 V is attributed to the reduction of the enzymatically produced hydrogen peroxide (see the reaction below). DP voltammograms illustrated in Fig. 5A manifest the enzymatic depletion of dissolved oxygen according to the course of the reaction

$$\text{Glucose} + O_2 \text{—GOx–>} \text{Gluconolactone} + H_2O_2$$

and define the time-span during which interference by the simultaneous electro reduction of dissolved oxygen is nil or negligible. The outstanding performance of GOx-FeSPC, with respect to that of FeSPC, for the detection of flunitrazepam in non-deoxygenated solutions of flunitrazepam in 0.1 M PBS pH 7 is illustrated in Fig. 5B. FeSPC

suffers by a large background signal over the potential range from −0.5 to −1.05 V, due to the electro reduction of dissolved oxygen, which hinders the detection of flunitrazepam at ca. −0.7 V even at concentrations as high as 5 μM. On the other hand, GOx-FeSPC provides analytically useful signals even in the presence of 1 μM flunitrazepam. As regards the peak at −0.5 V (reduction of hydrogen peroxide), the peak height is inversely proportional to the concentration flunitrazepam, indicating that the enzymatically produced H_2O_2 oxidizes the electrochemically generated hydroxylamine, in accordance with previous studies (Honeychurch et al., 2006). Remarkably, in situ enzymatic depletion of dissolved oxygen is also effective in a wide range of undiluted real-world samples (Pepsi cola®, Vodka, Whisky, Tequila, Gin, and Rum) of different acidity (pH 2.3–8.4), and alcohol content up to 40% v/v.

As illustrated in Fig. S5, GOx-FeSPC enables the detection of flunitrazepam at alcoholic and soft drinks spiked with flunitrazepam at concentrations considerably lower than those intended to instances of covert drug administration (25 mg mL^{-1}) (Salamone, 2001; Smith et al., 2013). The effect of the pH and alcohol content in each sample on the peak potential for the electro reduction of flunitrazepam along with the time required to achieve the lowest background signal are shown in Table S1.

Further studies aimed the applicability of GOx-FeSPC in a totally reagentless mode, that is, to avoid addition of glucose by the user. In this regard, we attempted to encapsulate the required amount of glucose in the form of sample dissolved hydrogel droplets. After the addition of 60 μL sample the glucose containing hydrogel droplets are dissolved yielding the concentration of glucose to be 10 mM. Among other tested polymers, sodium CMC at a concentration of 0.05% w/v was found to be the most suitable polymer for this purpose. In specific, i) the required amount of glucose is fully dissolved in CMC solution, ii) after the addition of glucose the polymer solution obtains a desired viscosity that facilitates the precise placement of the droplets in the space between the working and the auxiliary electrodes, iii) relative high contact angle GluHDs are not dispersed along the polystyrene substrate, thereby preventing contact of the polymer drops containing glucose with the GOx-modified surface of the working electrode, iv) GluHDs are readily dissolved upon the application of the various drop-volume aqueous or ethanol-containing samples, and most importantly, v) after their dissolution the response of the sensor is not suppressed. The response of GOx/GluHD-FeSPC sensor with respect to the concentration of CMC for the reagentless, drop-volume measurement of non-deoxygenated standard solutions of flunitrazepam over the concentration range 1–10 μM are shown in Fig. 6A. Inset graph shows the calibration plot, which was constructed by employing the optimum concentration of CMC (0.05% w/v). The equation for the straight line is $y/\mu A = (-0.238 \pm 0.079) + (0.357 \pm 0.13)$(flunitrazepam/μM) with a coefficient of determination $R^2 = 0.9956$, while the LOD (S/N 3) was found to be 0.7 μM. The reproducibility between different sensors was assessed by comparing the response of ten different GOx/GluHD-FeSPCs to a 5 μM flunitrazepam standard solution and it found to be < 12%. The sensors also displayed satisfactory storage stability when stored dry at 4 °C retaining more than 72% of their initial activity for at least two months.

3.4. Direct application of GOx/GluHD-FeSPC to real-world samples

DP voltammograms illustrated in Fig. 6B show the response of GOx/GluHD-FeSPCs at Pepsi cola®, Vodka, Whisky, Tequila, Gin, and Rum samples before and after spiking with 10 μM flunitrazepam. Each scan was conducted with an individual sensor, while the LODs (S/N 3) in each sample, that is, 2 μM (Pepsi cola®), and 1 μM (Vodka, Whisky, Tequila, Gin, and Rum) evidence the suitability of the designed disposable sensors for point-of-need screening of flunitrazepam. Considering that the addition of one pill Rohypnol® (1 mg flunitrazepam) in a portion of a strong alcoholic beverage (40 mL) or to a cocktail (80–120 mL) or to a soft drink (300–350 mL) results in a concentration level ranges from ca. 80–10 μM flunitrazepam, the proposed sensor holds promise as an effective analytical tool to prevent phenomena of covert drug administration.

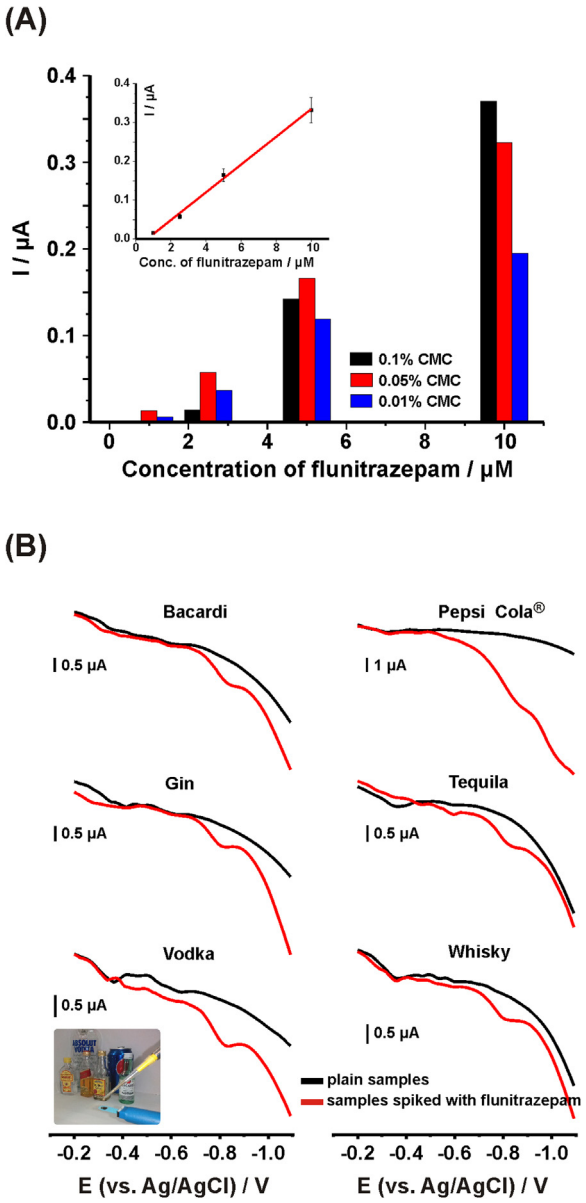

Fig. 6. (A) Comparative responses of GOx/GluHD-FeSPC fabricated by different concentrations of CMC and (inset graph) calibration plot for GOx/GluHD-FeSPC (0.05% w/v CMC) in non-deoxygenated 0.1 M PBS pH 7. (B) DP voltammograms of GOx/GluHD-FeSPCs to various untreated and undiluted soft drink and alcoholic beverages in the (black line) absence and in the (red line) presence of 10 μM flunitrazepam (For interpretation of the references to color in this figure legend, the reader is referred to the web version of this article).

4. Conclusions

This work employs low-cost, lab-on-a-screen-printed electrochemical cells that have been successfully used for the direct, cathodic voltammetric detection of flunitrazepam in a wide range of untreated and undiluted spiked samples (Pepsi cola®, Vodka, Whisky, Tequila, Gin, and Rum) of different acidity (pH 2.3–8.4), and alcohol content up to 40% v/v.

The designed lab-on-a-screen-printed electrochemical cell holds also

promise for use in point-of-care applications. Besides it has been designed to operate with a small volume of sample (drop-volume), oxygen interference, a common obstacle in cathodic voltammetric measurements, is effectively alleviated by an in situ deoxygenation process based on GOx-glucose enzyme reaction, which crucially, works effectively over a wide range of pH values and high ethanol content spirits.

By employing the spark discharge method, an extremely simple, fast (30 sparks takes ca. 20–30 s to be applied) and totally "green" method, which is conducted in the absence of any organic solvents or other liquids (Riman et al., 2017, 2015; Tabrizi et al., 2009), GOx/GluHD-FeSPCs were modified with Fe_xO_y nanoparticles, which proved to be excellent electro catalyst for the electro reduction of flunitrazepam.

GOx/GluHD-FeSPCs offer limits of detection within the dosage range intended to be found in covert drug administration events, and, therefore, holds promise as an effective analytical tool for the point-of-need screening of flunitrazepam by coupling the designed sensors with hand-held electroanalytical devices.

The development of analytical devices enabling the interference free electro reduction of nitrocompounds in the presence of dissolved oxygen, offers a wide scope of applications, and advanced utility for the development of methods intended to be used for point-of-care applications where sample deoxygenation is a serious limitation.

Conflicts of interest

There are no conflicts to declare.

Declaration of interests

None.

Appendix A. Supporting information

Supplementary data associated with this article can be found in the online version at doi:10.1016/j.bios.2019.03.001.

References

Amir, L., Waisman, Y., 2006. Isr. J. Emerg. Med. 6, 62–66.
Baciu, T., Botello, I., Borrull, F., Calull, M., Aguilar, C., 2015. TrAC - Trends Anal. Chem. 74, 89–108.
Barrett, A.M., Walshe, K., Kavanagh, P.V., McNamara, S.M., Moran, C., Burdett, J., Shattock, A.G., 1999. Addict. Biol. 4, 81–87.
Bermejo, E., Zapardiel, A., Pérez, J.A., Huerta, A., Hernández, L., 1993. Talanta 40, 1649–1656.
Beynon, C.M., McVeigh, C., McVeigh, J., Leavey, C., Bellis, M.A., 2008. Trauma, Violence, Abus. 9, 178–188.
Beynon, C.M., Sumnall, H.R., McVeigh, J., Cole, J.C., Bellis, M.A., 2006. Addiction 101, 1413–1420.
Bu, Y., Zhong, Q., Xu, D., Tan, W., 2013. J. Alloy. Compd. 578, 60–66.
Council of Europe, 2006. Council of Europe, Parliament Assembly, Doc. 11038 (2006, October 2). Sexual assaults linked to date-rape drugs. ⟨http://www.assembly.coe.int/Documents/WorkingDocs/2006/EDOC11038.pdf⟩. (Accessed December 2018).
D'Aloise, P., Chen, H., 2012. Sci. Justice 52, 2–8.
Dasgupta, A., 2017. Alcohol, Drugs, Genes and the Clinical Laboratory, first ed. Academic Press, New York.
Dinis-Oliveira, R.J., Magalhães, T., 2013. Toxicol. Mech. Methods 23, 471–478.
DrinkSavvy, 2018. ⟨http://drinksavvy.com/⟩. (Accessed December 2018).
Drug-Induced Rape Prevention and Punishment Act, 1996. H.R.4137, 104th Congress.
Executive Office of the President, 2003. Rohypnol. Executive Office of the President, Office of National Drug Control Policy, Washington, DC.
Garcia-Gutierrez, E., Lledo-Fernandez, C., 2013. Chemosensors 1, 68–77.
Garcia-Gutierrez, E., Lledo-Fernandez, C., Raspeig, del, Vicente del Raspeig Alicante, S., 2013. Univ. J. Chem. 1, 121–127.
Graat, P.C.J., Somers, M.A.J., 1996. Appl. Surf. Sci. 100–101, 36–40.
Honeychurch, K.C., Hart, J.P., 2008. J. Solid State Electrochem. 12, 1317–1324.
Honeychurch, K.C., Smith, G.C., Hart, J.P., 2006. Anal. Chem. 78, 416–423.
Huang, C.W., Jen, H.P., Wang, R., De, Hsieh, Y.Z., 2006. J. Chromatogr. A 1110, 240–244.
Kokkinos, C., Prodromidis, M., Economou, A., Petrou, P., Kakabakos, S., 2015a. Anal. Chim. Acta 886, 29–36.
Kokkinos, C., Prodromidis, M., Economou, A., Petrou, P., Kakabakos, S., 2015b. Electrochem. Commun. 60, 47–51.
LeBeau, M., Mozayani, A., 2001. Drug-Facilitated Sexual Assault: A Forensic Handbook, first ed. Academic Press, Washington.
Leesakul, N., Pongampai, S., Kanatharana, P., Sudkeaw, P., Tantirungrotechai, Y., Buranachai, C., 2012. Luminescence 28, 76–83.
Mattila, M.A.K., Larni, H.M., 1980. Drugs 20, 353–374.
McNeill, D., 2018. The IrishTimes, July 10. Woman's fight highlights rape taboo in Japan. ⟨https://www.irishtimes.com/news/world/asia-pacific/woman-s-fight-highlights-rape-taboo-in-japan-1.3559299⟩. (Accessed December 2018).
Miller, C.T., Armstrong, K., 2018. A False Report: A True Story of Rape in America, first ed. Crown, New York.
Mullins, M.E., 1999. Acad. Emerg. Med. 6, 966–968.
Núñez-Vergara, L.J., Bollo, S., Olea-Azar, C., Navarrete-Encina, P.A., Squella, J.A., 1997. J. Electroanal. Chem. 436, 227–238.
Oelshlager, H., 1983. Bioelectrochem. Bioenergetics 10, 25–36.
Riman, D., Jirovsky, D., Hrbac, J., Prodromidis, M.I., 2015. Electrochem. Commun. 50, 20–23.
Riman, D., Spyrou, K., Karantzalis, A.E., Hrbac, J., Prodromidis, M.I., 2017. Talanta 165, 466–473.
Salamone, S.J., 2001. Benzodiazepines and GHB: Detection and Pharmacology. Humana Press, New York.
Samyn, N., De Boeck, G., Cirimele, V., Verstraete, A., Kintz, P., 2002. J. Anal. Toxicol. 26, 211–215.
Schwartz, R.H., 1998. Clin. Pediatr. 37, 321–322.
Smith, J.P., Metters, J.P., Kampouris, D.K., Lledo-Fernandez, C., Sutcliffe, O.B., Banks, C.E., 2013. Analyst 138, 6185–6191.
Tabrizi, N.S., Ullmann, M., Vons, V.A., Lafont, U., Schmidt-Ott, A., 2009. J. Nanopart. Res. 11, 315–332.
U.S. Department of justice, 2017. U.S. Department of justice, Community Outreach and Prevention Support Section, Drug-Facilitated Sexual Assault ⟨https://www.dea.gov/sites/default/files/2018-07/DFSA_0.PDF⟩. Accesed December 2018.
Walby, S., Allen, J., 2004. Domestic Violence, Sexual Assault and Stalking: Findings from the British Crime Survey: Home Office Research Study 276 Home Office Research, Development and Statistics Directorate, London.
Webb, R., Doble, P., Dawson, M., 2007. Electrophoresis 28, 3553–3565.
Weir, E., 2001. Can. Med. Assoc. J. 165, 80–85.
WHO, 2003. Guidelines for Medico-Legal Care for Victims of Sexual Violence Guidelines for Medico-Legal Care for Victims of Sexual Violence. World Health Organization, Geneva.
Wilhelm, M., Battista, H.J., Obendorf, D., 2000. J. Chromatogr. A 897, 215–225.
Wu, L.T., Schlenger, W.E., Galvin, D.M., 2006. Drug Alcohol Depend. 84, 102–113.